Optical investigations on the biaxial smectic-*A* phase of a bent-core compound

S. T. Wang,[1] X. F. Han,[1,*] A. Cady,[1,*] Z. Q. Liu,[1] A. Kamenev,[1] L. Glazman,[1] B. K. Sadashiva,[2] R. Amaranatha Reddy,[2] and C. C. Huang[1]

[1]*School of Physics and Astronomy, University of Minnesota, Minneapolis, Minnesota 55455, USA*

[2]*Raman Research Institute, C. V. Raman Avenue, Bangalore 560080, India*

(Received 25 September 2003; published 21 December 2004)

Several unique optical properties have been obtained from freestanding films of a bent-core compound. Our experimental results indicate the existence of the antiferroelectric biaxial smectic-*A* (Sm *A*) phase. The critical exponent associated with the biaxiality through the uniaxial–antiferroelectric biaxial Sm *A* transition has been measured to be 0.82 ± 0.04, which is in good agreement with our theoretical calculation. Our theoretical advances further demonstrate that the critical behavior of the optical biaxiality with the order parameter being a vector is described by the secondary-order parameter of the three-dimensional *XY* model. We also observe a remarkable even–odd layering effect exhibited by the surface layers of freestanding films under an applied electric field (≈ 20 V/cm) in the film plane.

DOI: 10.1103/PhysRevE.70.061705 PACS number(s): 61.30.Eb, 61.30.Cz, 77.84.Nh

I. INTRODUCTION

In a biaxial smectic-*A* (Sm *A*) phase, one of the principal axes is along the layer normal ($\hat{z}$). The other two inequivalent orthogonal principal axes are in the layer plane. Depending on whether $\hat{z}$ is a twofold rotational axis or not of the biaxial Sm *A*, the order parameter of the uniaxial–biaxial Sm *A* transition is a director or vector, respectively. For instance, the biaxial Sm *A* (the C_M) phase predicted by de Gennes [1] and reported in Refs. [2–4] has a twofold rotational symmetry around $\hat{z}$ [see Fig. 1(a)] while the one (the C_P) predicted by Brand *et al.* [5] and evidenced in bulk samples in Ref. [6] does not [see Fig. 1(b)]. The C_P has C_{2v} symmetry and allows the existence of a spontaneous electric polarization along the rotational axis which is in the layer plane. The C_P can be ferroelectric or antiferroelectric, depending on the molecular arrangements in the successive layers.

In this paper, we report null transmission ellipsometry (NTE) [7] studies on freestanding films of a bent-core compound 1g14. Its molecular structure and phase sequence are given in Fig. 1(c). The biaxial and uniaxial Sm *A* phases are named Sm A_{db} and Sm A_d, respectively, due to the partial bilayer molecular packing [8]. The enthalpy associated with the Sm A_{db}-Sm A_d transition is 0.13 kJ/mol [8], which is relatively small and indicates that the transition is either weakly first order or continuous. Our investigations demonstrate that the Sm A_{db} is the antiferroelectric C_P phase. From our high-resolution data obtained from thick freestanding films, the critical exponent (β_2) of the biaxiality, the difference of the dielectric constants in the layer plane through the uniaxial Sm *A*–antiferroelectric C_P transition has been found to be 0.82 ± 0.04. The value of β_2 agrees well with our theoretical calculation. We show that the critical behavior of the optical biaxiality is described by the secondary-order parameter of the three-dimensional (3D) *XY* model if the order parameter is a vector. This is in contrast with the transitions described by a director, where the optical biaxiality is proportional to the leading order parameter. Moreover, we report a surface transition occurring in films of even number of layers (N) under an applied in-plane electric field (E) on the order of 20 V/cm. Such a surface transition does not occur in films of odd N.

II. EXPERIMENTAL METHODS

In our NTE, Δ measures the phase difference between the $\hat{p}$ and $\hat{s}$ components of the incident light with wavelength 633 nm to produce linearly polarized transmitted light. Ψ describes the polarization angle of this linearly polarized

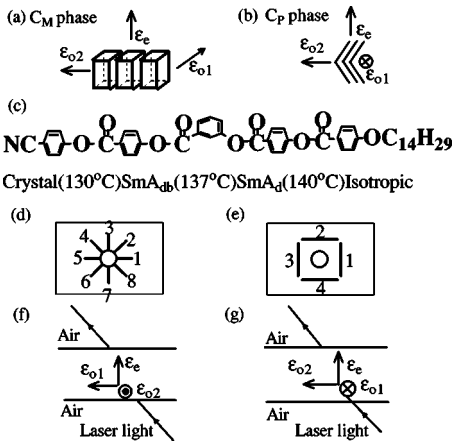

FIG. 1. (a) and (b) schematically show the molecular packing, the principal axes, and the dielectric constants of the C_M and C_P phases. (c) presents the chemical structure and phase sequence of 1g14. The bend in the molecule is determined by the bonds to the central benzene ring. To save space, the molecule is drawn straight. (d) and (e) depict the film plates used in our studies. (f) and (g) show the two different geometries of the biaxial ellipsoid relative to the incident plane.

*Present address: Advanced Photon Source, Argonne National Laboratory, Argonne, IL 60439.

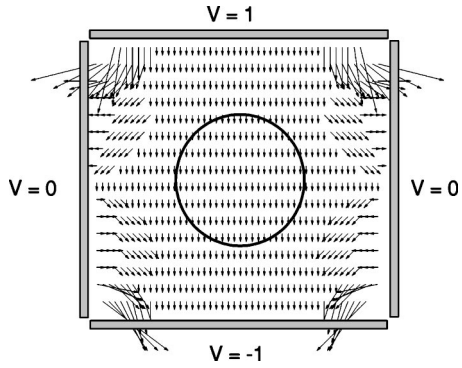

FIG. 2. E map from numerical simulations for the film plate with four electrodes. The potentials of four electrodes in arbitrary units are labeled beside them, respectively. The middle circle indicates the position of the opening where freestanding films suspend.

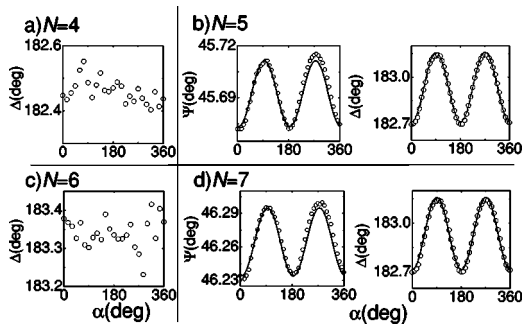

FIG. 3. Ψ and Δ versus α from four-, five-, six-, and seven-layer films (a)–(d) under $|E|=22$ V/cm at $T_c-T=3.2$ K in the Sm A_{db} phase. Ψ from four- and six-layer films are not shown to save space. The solid lines in (b) and (d) are fits to the data.

light. Our resolution for Ψ and Δ is 0.002°. Details of our NTE are described in a recent paper [9].

In our studies, a small dc E of about 20 V/cm is applied in the layer plane. If there is a nonzero net electric polarization in the layer plane, the alignment of the electric polarization by E can create a single domain larger than our laser beam. Note that the range of our E strength is large enough to align the molecular orientation but is too small to change the intrinsic properties of liquid crystals [10]. Moreover, the effect due to the coupling between the dielectric anisotropy [11] and such small E can be ignored because the coupling is of higher order of E. Upon reducing E field to zero, the films in the Sm A_{db} phase will develop multidomains due to thermal fluctuations.

Two kinds of film plates depicted in Figs. 1(d) and 1(e) have been used in our studies. For the one in Fig. 1(d), the voltages applied to the electrodes are $V_m=V\cos[45°\times(m-1)-\alpha]$, where m ranges from 1 to 8. In this way, a uniform rotatable E with azimuthal angle α can be created in the center of the hole where our laser beam passes through. When $\alpha=90°$ or 270° the direction of E is perpendicular to the incident plane defined by the wave vector of the laser light and $\hat{z}$. The film plate illustrated in Fig. 1(e) allows us to apply E parallel or perpendicular to the incident plane. For instance, by setting V, 0, $-V$, and 0 to electrode 1, 2, 3, and 4, respectively, E pointing from the midpoint of electrode 1 to the midpoint of electrode 3 can be created in the center of the hole. The diameter of the hole on the film plate with eight and four electrodes was 4.5 and 2.0 mm, respectively. The distance between the parallel electrodes of the film plate with four electrodes was 4.5 mm. The area of our laser spot on films is less than 0.5 mm^2.

A simulation of E in the film plate with four electrodes is shown in Fig. 2. At the corners and the places that are close to two electrodes with zero potential, E is curved and strong. However, in the area where the films locate (in the circle), E is uniform and weak. The simulation of E for the film plate with eight electrodes can be found in Ref. [9]. It also shows that E is uniform in the region where our film is located. These simulations have demonstrated that the deviation of the direction of E from the desired direction in the area of the laser spot for both types of film plates is less than 1°. Both types of film plates work fine for applying E parallel or perpendicular to the incident plane. We compared the results obtained using both film plates and found out they are the same. These two film plates have very different boundary conditions and yield different orientation as well as strength of E near the boundaries. The consistency of our experimental data obtained from the centers of the film holes of two different film plates demonstrates that the effect of boundary E is small and can be ignored.

In freestanding films the thickness is quantized in integer numbers of layers. For freestanding films in the uniaxial Sm A phase, there are analytical solutions for Ψ and Δ as a function of the dielectric constants along $\hat{z}$ (ε_{e0}) and in the layer plane (ε_o), the layer spacing (h_0), and N [9,12]. By measuring Ψ and Δ of many films with different thicknesses and fitting the data with analytical calculations, ε_{e0}, ε_o, and h_0 (and N of these films) can be obtained [13]. After the optical parameters are known, N of any film can be determined. For 1g14, at 1 K above the Sm A_{db}-Sm A_d transition temperature (T_c) in the uniaxial Sm A_d phase, about 30 films were prepared and ε_{e0}, ε_o, h_0 were acquired to be $(1.635\pm0.003)^2$, $(1.515\pm0.001)^2$, and 5.21 ± 0.03 nm, respectively. Our layer spacing measurement agrees well with the result obtained from x-ray diffraction [8,14].

III. EXPERIMENTAL RESULTS AND DISCUSSION

A. The biaxial Sm A phase

At $T_c-T=3.2$ K in the Sm A_{db} phase, rotations of E on many films were performed by using the film plate with eight electrodes. The scattering nature of the data obtained from films of even N indicates that there is no detectable net electric polarization in the film plane while data from films of odd N suggest that there is a net polarization. This even–odd layering effect is typical for antiferroelectric samples in which the direction of the electric polarization alternates from layer to layer [15]. Data acquired from four-, five-, six-, and seven-layer films are shown in Fig. 3.

More importantly, the data obtained from films of odd N strongly suggest that neither Ψ nor Δ changes upon reversal of E; namely, the optical properties of the film are invariant upon such reversal. Since the molecules are rotated around $\hat{z}$

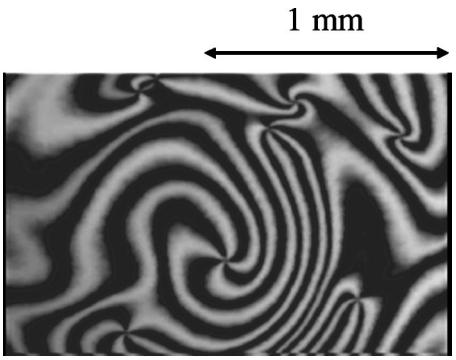

FIG. 4. This picture shows the image captured from an odd-layer film with $E=0$ at $T=135$ °C under crossed polarizers. Seven ± 1 point defects can be identified in this photo.

by 180° upon reversal of E, the invariance means that $\hat{z}$ is one of the principal axes of the dielectric tensor of films of odd N. Thus, $\hat{z}$ is also one principal axis for a single layer. In addition, the variation of Ψ and Δ as a function of α suggests that the other two principal axes of the dielectric tensor must be inequivalent. Therefore, these demonstrate that the Sm A_{db} phase is the antiferroelectric C_P phase.

Numerical simulations of the data obtained under rotations of E were done with the 4×4 matrix method [12]. ε_e, ε_{o1}, ε_{o2}, and the layer spacing (h) used in the simulation of Figs. 3(b) and 3(d) are 1.675^2, 1.5105^2, 1.5195^2, 5.14 nm and 1.700^2, 1.510^2, 1.520^2, 5.16 nm, respectively. The respective parameters to fit the data obtained from 121- and 43-layer films at 3.8 K below T_c are 1.650^2, 1.511^2, 1.519^2, 5.16 nm, and 1.650^2, 1.511^2, 1.519^2, 5.19 nm. These parameters indicate that the variations of h and the dielectric constants from the values in the Sm A_d phase are small when temperature is close to T_c. This will be useful for later discussions.

Upon removing the applied E, the Schlieren texture with only $s=\pm 1$ point defects characterized by four dark brushes, is visible by the reflected optical microscopy under crossed polarizers. One of such pictures from an odd-layer film taken at 135 °C is shown in Fig. 4. From 15 different films with $E=0$, we always observe several $s=\pm 1$ point defects in each film and did not observe any $s=$half-integer point defect. Some films were prepared and observed without applied E. Thus the molecular arrangement below T_c is truly a biaxial C_p phase.

B. Critical exponent associated with the biaxiality

Our next goal is to study the temperature dependence of the biaxiality $\varepsilon_{o2}-\varepsilon_{o1}$. If one of the principal axes of the dielectric tensor in the layer plane of the Sm A_{db} phase is in the incident plane, as is depicted in Figs. 1(f) and 1(g), there are analytical solutions for Ψ and Δ following Refs. [12] and [9]. If the dielectric constants are uniform along $\hat{z}$, the two configurations in Figs. 1(f) and 1(g) can be achieved by applying E perpendicular and parallel to the incident plane, respectively, to films of odd N because they have a nonzero net electric polarization. Let Δ_p and Δ_i denote Δ for the configurations in Figs. 1(f) and 1(g), respectively. Also

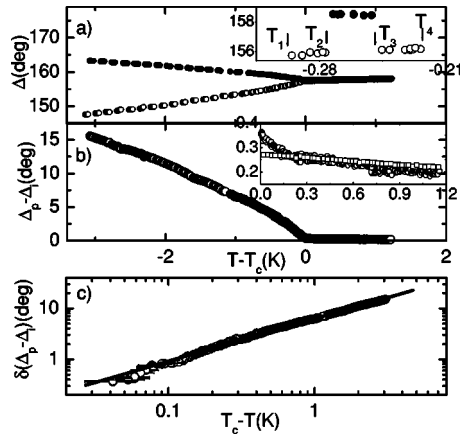

FIG. 5. (a) shows the temperature dependence of Δ from a 321-layer film under two directions of E with $|E|=25$ V/cm obtained upon heating. Open and solid circles are for E parallel and perpendicular to the incident plane, respectively. The inset shows the data over a small temperature window close to T_c. (b) presents $\Delta_p-\Delta_i$ of the data in (a). The inset highlights $\Delta_p-\Delta_i$ above T_c with circles for the 321-layer film. The squares in the inset are $\Delta_p-\Delta_i$ from a seven-layer film. (c) shows $\delta(\Delta_p-\Delta_i)$ versus T_c-T in a log to log scale for the 321-layer film after the effect due to surface layers is subtracted below T_c. Symbols are results and the solid line is a linear fit. The error bar of temperatures is also displayed in (c). Due to the fact that the direction of E was switched upon heating, the error bar is 30 and 15 mK below and above $T_c-0.8$ K, respectively.

δ_{o1}, δ_{o2}, δ_h, and δ_e indicate the temperature variation of ε_{o1}, ε_{o2}, h, and ε_e from the values (ε_o, ε_o, h_0, and ε_{e0}, respectively) in the uniaxial Sm A phase. Within the temperature range we studied δ_{o1}, δ_{o2}, δ_h, and δ_e are small. We have

$$\begin{aligned}\Delta_p-\Delta_i &\equiv \Delta(\varepsilon_{o2},\varepsilon_{o1},h,\varepsilon_e)-\Delta(\varepsilon_{o1},\varepsilon_{o2},h,\varepsilon_e)\\ &\equiv \Delta(\varepsilon_o+\delta_{o2},\varepsilon_o+\delta_{o1},h_0+\delta_h,\varepsilon_{e0}+\delta_e)\\ &\quad -\Delta(\varepsilon_o+\delta_{o1},\varepsilon_o+\delta_{o2},h_0+\delta_h,\varepsilon_{e0}+\delta_e)\\ &\approx [\Delta_1(\varepsilon_o,\varepsilon_o,h_0,\varepsilon_{e0})-\Delta_2(\varepsilon_o,\varepsilon_o,h_0,\varepsilon_{e0})](\varepsilon_{o2}-\varepsilon_{o1})\end{aligned}$$

where Δ_1 and Δ_2 are the first-order derivatives of Δ with respect to the first and second variable, respectively. In the approximation, only the first order terms of the Taylor expansion are taken into account. From the analytical solutions, we know that $\Delta_1-\Delta_2$ is nonzero for physically reasonable parameters. Thus, $\Delta_p-\Delta_i$ is proportional to $\varepsilon_{o2}-\varepsilon_{o1}$.

Temperature ramps were conducted on many films of odd N with both film plates. Although the films were prepared and kept in an inert gas environment, we detected a noticeable 0.50 mK/min drift in T_c due to sample thermal degradation. To minimize the complications caused by such an effect, we acquired the data in the following procedures. During temperature ramps the direction of E was switched every 5 min between being perpendicular and parallel to the incident plane. The temperature ramping rate was set to be 12 mK/min below $T_c-0.8$ K and 6 mK/min above that temperature. Typical data obtained from a 321-layer film are presented in Fig. 5(a). As the inset of Fig. 5(a) shows, between T_2 and T_3, the direction of E is perpendicular to the incident plane. We do not have the data for E in the incident

plane. However, since this window is small (0.03 K in the inset), the data are determined by linear interpolation of the data over T_1 and T_2, and T_3 and T_4. A similar procedure has been applied to the data with E perpendicular to the incident plane. Then the difference as a function of temperature can be taken and the results are presented in Fig. 5(b). The inset of Fig. 5(b) shows $\Delta_p-\Delta_i$ above T_c with circles for the 321-layer film. The nonzero $\Delta_p-\Delta_i$ is due to the biaxiality in surface layers with enhanced ordering. A linear fit is done for the results above $T_c+0.3$ K and the effect due to surface layers is subtracted from the results in Fig. 5(b). The final results $\delta(\Delta_p-\Delta_i)$ below T_c are presented in Fig. 5(c) in a log-log plot. A linear function provides an excellent fit over about two decades in the reduced temperature scale with a slope of $\beta_2=0.83$.

As briefly mentioned above, the effect of surface layers on $\Delta_p-\Delta_i$ is assumed to be linear with temperature for simplicity. For comparison, $\Delta_p-\Delta_i$ from a seven-layer film above T_c is also presented in the inset of Fig. 5(b) with squares. As shown in the inset, $\Delta_p-\Delta_i$ from 321- and seven-layer films coincide at temperature 0.2 K above T_c. This indicates that there are at most seven surface layers which differ from the interior layers. Thus the error due to the surface layers on β_2 from the 321-layer film is less than 3%.

Similarly, β_2 obtained from 587-, 597-, and 151-layer films is 0.78, 0.84, and 0.83, respectively. The average is 0.82 and the error bar is ≈ 0.04 to cover all the results. This value is for sure more than twice the order parameter exponent of the 3D XY model: $\beta\approx 0.35$. In the following, we demonstrate that the optical biaxiality in the C_P phase does not scale with the order parameter exponent β, but rather with a different and independent critical exponent $\beta_2 \geqslant 2\beta$. Here the equality takes place only above the upper critical dimension ($d=4$), while in 3D samples this is a strict inequality. This statement should be contrasted with the behavior of the biaxial C_M phase, where the optical biaxiality is proportional to the leading order parameter.

The orientation of molecule $\vec{l}$ in liquid crystal layer m can be characterized by a vector of dipole moment $\mathbf{d}_{\vec{l}m}$. In the C_P phase, the dipole nature of molecules and the character of ordering tell us that the order parameter for the transition into the C_P state is $\vec{\Phi}\propto(-1)^m\mathbf{d}_{\vec{l}m}$ and $\propto\mathbf{d}_{\vec{l}m}$ for the antiferroelectric and ferroelectric C_P, respectively. In terms of $\vec{\Phi}(\mathbf{r})$, the transition is described by an anisotropic 3D XY model. The orientation of the principal axes of the dielectric tensor $\hat{\varepsilon}(\mathbf{r})$ is related to the orientation of $\vec{\Phi}(\mathbf{r})$, and thus fluctuates together with it. At optical frequency, in terms of the angle $\phi(\mathbf{r})$ between this vector and a direction in the laboratory frame $\hat{\varepsilon}=\hat{O}^T(\phi)\mathrm{diag}\{\varepsilon_1,\varepsilon_2\}\hat{O}(\phi)$. Here $\hat{O}(\phi)$ is an azimuthal rotation matrix of a molecule, and $\varepsilon_{1,2}$ are the principal dielectric constants of a fully-ordered state. The biaxiality is characterized by the difference of the observed principal values of the dielectric tensor $\varepsilon_{o1}-\varepsilon_{o2}=(\varepsilon_1-\varepsilon_2)\langle\cos 2\phi\rangle \propto[\langle(\vec{n}\cdot\vec{\Phi})^2\rangle-1/2]$, with $\vec{n}$ being a unit vector in the direction of the spontaneous polarization.

The critical exponent β_2 of $\langle(\vec{n}\cdot\vec{\Phi})^2\rangle$ cannot be expressed in terms of the leading-order parameter $\langle\vec{n}\cdot\vec{\Phi}\rangle$ of the critical exponent β, but, like β, it may be evaluated by the conventional renormalization group procedure [16,17]. For that purpose, we add a perturbation $w\langle(\vec{n}\cdot\vec{\Phi})^2\rangle$ to the conventional Hamiltonian of the XY model,

$$H=\int d^dx[K(\vec{\nabla}\cdot\vec{\Phi})^2+t\vec{\Phi}^2+u(\vec{\Phi}^2)^2],$$

and use the $4-\epsilon$ expansion technique. The straightforward one-loop renormalization group equations for the coupling constants read

$$dt/d\xi=2t-32tu-8wu,$$

$$du/d\xi=\epsilon u-80u^2,$$

$$dw/d\xi=2w-16wu.$$

The first two equations here are fairly standard [18], while the last one is needed to find the critical exponent β_2. The fixed point to the linear order in ϵ is given by $u^*=\epsilon/80$ and $t^*=w^*=0$, and the relevant fixed point eigenvalues are $y_t=2-2\epsilon/5$; and $y_w=2-\epsilon/5$. According to the standard scaling arguments [18] the order parameter critical exponent is given by $\beta_2=(d-y_w)/y_t$, which leads to $\beta_2=1-\epsilon/5$. Notice that to the same order in ϵ the leading exponent is [18] $\beta=\frac{1}{2}(1-3\epsilon/10)$ and therefore, indeed, $\beta_2>2\beta$ for $d<4$, the upper critical dimensionality for the XY model. Employing two-loop results from Ref. [17], one finds $\beta_2=1-\epsilon/5+3\epsilon^2/50+O(\epsilon^3)$. Substituting finally $\epsilon=1$, one may estimate the exponent as $\beta_2\approx 0.86$, in a very good agreement with our experimental finding $\beta_2=0.82\pm 0.04$.

Our β_2 also agrees well with the critical exponent of the second harmonic-order parameter determined from the x-ray diffraction intensity profile through the Sm C to Sm I transition [16]. Unlike previous measurements [16], where the whole set of exponents $\beta_n\,(1\leqslant n\leqslant 7)$ were extracted from the same data, the optical biaxiality is exclusively related to the secondary-order parameter $\langle(\vec{n}\cdot\vec{\Phi})^2\rangle$ of the C_P, and therefore provides a direct access to the value of β_2. This discussion clarifies the difference between the C_P and C_M phases. In the latter case the leading order parameter is $\langle\cos 2\phi\rangle$ (since $\langle\cos\phi\rangle$ is identically zero by the director nature of the order parameter). Thus, the optical biaxiality is proportional to the leading order parameter [19].

C. Even–odd layering effect on the surface layers

In addition to the critical exponent, the surface layers of freestanding films of 1g14 also show a remarkable even–odd layering effect under E on the order of 20 V/cm. The temperature dependence of Δ obtained upon heating from four films using the film plate with eight electrodes under $|E|=22$ V/cm are presented in Fig. 6. From the data, Δ at $\alpha=90°\,(\Delta_{90})$ is always larger than Δ at $\alpha=0°\,(\Delta_0)$ for films of odd N. For films of even N, there is a temperature window in which $\Delta_{90}<\Delta_0$. At high enough temperatures, like the data obtained from films of odd N, $\Delta_{90}>\Delta_0$.

The observation can be explained by the following model. As temperature approaches T_c from below, the interior layers

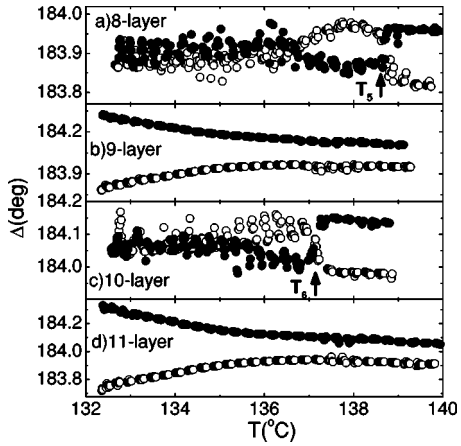

FIG. 6. Δ versus temperature obtained upon heating at 30 mK/min from eight-, nine-, ten-, and 11-layer films (a)–(d). During heating, α was switched between 0° (open circles) and 90° (solid circles) every 5 min. The strength of E was 22 V/cm for all the films.

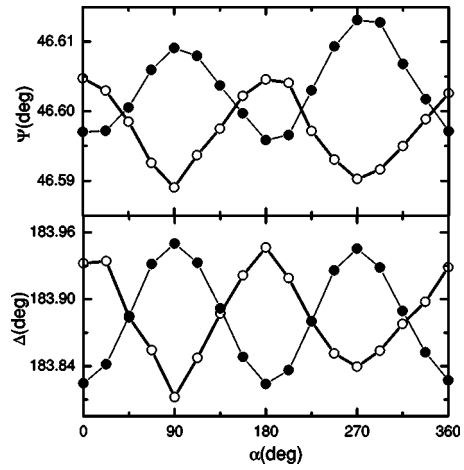

FIG. 8. Ψ and Δ versus α obtained from an eight-layer film at 2.5 K above T_c under $E=4.5$ V/cm (open circles) and $E=20$ V/cm (solid circles). The solid lines are guides to the eye.

gradually become uniaxial. However, due to the enhanced surface ordering, the surface layers can be biaxial even at temperatures above T_c. In films of odd N, the polarizations of the two surface layers are parallel in the Sm A_{db} phase and remain so as temperature increases under E. A model of films of odd N is schematically depicted in Fig. 7(a) with a three-layer film as an example. $\mathbf{b}_1$ and $\mathbf{b}_2$ represent the two $\mathbf{b}$ vectors (and the two polarizations) of the two surface layers. The straight rod in the right cartoon conveys that this layer becomes uniaxial. The result is that on average the dielectric constant along E ($\varepsilon_\parallel$) is always larger than the one perpendicular to E ($\varepsilon_\perp$) and Δ_{90} is always larger than Δ_0 as long as there is some polarization and biaxiality in the surface layers.

However, for films of even N, the polarization of the two surface layers are antiparallel in the Sm A_{db} phase. As temperature increases, the coupling of the surface layers through the interior layers becomes weak. A small E can slightly distort the ground state, leading to the structure shown in Fig. 7(b.1). The angle between $\mathbf{b}_1$ and E is equal to the one between $\mathbf{b}_2$ and E. The two angles are slightly smaller than 90°. This arrangement of the two surface polarizations gives a net polarization along the direction of E. In this arrangement, $\varepsilon_\parallel$ is smaller than $\varepsilon_\perp$. Thus, $\Delta_{90}<\Delta_0$ is expected. As temperature continues to increase, the angle between $\mathbf{b}_1$ and $\mathbf{b}_2$ becomes smaller. Eventually, they are forced to be parallel to each other. The result is $\varepsilon_\parallel>\varepsilon_\perp$ and $\Delta_{90}>\Delta_0$. What occurs in even-layer films viewed along a direction perpendicular to $\hat{z}$ and E is also schematically shown in Fig. 7(b.2). This argument yields a satisfactory explanation of our data shown in Fig. 6.

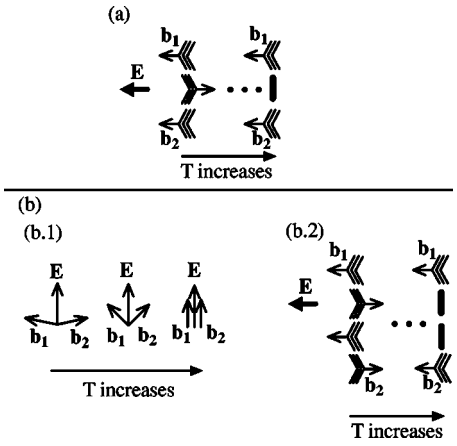

FIG. 7. (a) and (b) schematically depict what occurs in films with odd and even layers under E as temperature is increased from the biaxial to uniaxial Sm A phase, respectively. In (a) and (b.2), the viewing direction is perpendicular to $\hat{z}$ and E. In (b.1) the viewing direction is along $\hat{z}$. The straight rods in (a) and (b.2) convey that these layers become uniaxial.

At given temperature, increasing the strength of E can also induce the surface transition in even-layer films. Data obtained from an eight-layer film under two strengths of E at $T-T_c=2.5$ K is presented in Fig. 8. Under $E=4.5$ V/cm, both Ψ and Δ as a function of α exhibit a W-like curve, which suggests that $\varepsilon_\parallel<\varepsilon_\perp$. Under $E=20$ V/cm, the curves of both Ψ and Δ as a function of α are M-like, which indicates that $\varepsilon_\perp<\varepsilon_\parallel$. This behavior can be explained by the above argument, namely, under $E=4.5$ V/cm, the angle between $\mathbf{b}_1$ and $\mathbf{b}_2$ is close to 180° while under $E=20$ V/cm, the angle is close to 0°.

Another point is that in Figs. 6(a) and 6(c), there is a temperature at which Δ_0 and Δ_{90} cross (indicated as T_5 and T_6, respectively). T_5 is 2° higher than T_6. This is because the coupling of two surface layers is stronger in eight-layer films than in ten-layer films. It needs more thermal fluctuation to break the coupling of two surface layers in eight-layer films than ten-layer films under the same strength of E.

IV. CONCLUSION

In summary, NTE results obtained from freestanding films are presented to demonstrate the existence of the antiferroelectric C_P phase. The critical exponent associated with the biaxiality has been measured to be $\beta_2=0.82\pm0.04$. This

value has been identified (and compared favorably with the second-order ϵ expansion) as secondary-order parameter exponent of the 3D *XY* model. We believe that our result is the first direct measurement of β_2. We also point out the crucial difference with the critical behavior of the optical biaxiality in the C_M phase, which is governed by the leading order parameter. Unusual surface behavior depending on whether N is even or odd under an applied E has been presented and explained.

ACKNOWLEDGMENTS

We are grateful to Professor H. R. Brand and Professor A. Aharony for valuable discussions. The research was supported in part by the National Science Foundation, Solid State Chemistry Program under Grants No. DMR-0106122, No. DMR02-37296, and No. EIA02-10736. X.F.H. wishes to acknowledge financial support from the Stanwood Johnston Memorial Foundation at the University of Minnesota.

[1] P. G. de Gennes, *The Physics of Liquid Crystals* (Clarendon, Oxford, 1974), p. 279.

[2] H. F. Leube and H. Finkelmann, Makromol. Chem. **191**, 2707 (1990); **192**, 1317 (1991).

[3] R. Pratibha, N. V. Madhusudana, and B. K. Sadashiva, Science **288**, 2184 (2000).

[4] T. Hegmann, J. Kain, G. Pelzl, S. Diele, and C. Tschierske, Angew. Chem., Int. Ed. **40**, 887 (2001).

[5] H. R. Brand, P. E. Cladis, and H. Pleiner, Macromolecules **25**, 7223 (1992); Eur. Phys. J. B **6**, 347 (1998).

[6] A. Eremin, S. Diele, G. Pelzl, H. Nádasi, W. Weissflog, J. Salfetnikova, and H. Kresse, Phys. Rev. E **64**, 051707 (2001).

[7] R. M. A. Azzam and N. M. Bashara, *Ellipsometry and Polarized Light* (North-Holland, Amsterdam, 1989).

[8] B. K. Sadashiva, R. Amaranatha Reddy, R. Pratibha, and N. V. Madhusudana, J. Mater. Chem. **12**, 943 (2002).

[9] D. A. Olson, X. F. Han, P. M. Johnson, A. Cady, and C. C. Huang, Liq. Cryst. **29**, 1521 (2002).

[10] The critical E to induce the antiferroelectric-ferroelectric transition of liquid crystals is ≈ 1 V/μm (e.g., see Ref. [6]). The largest electroclinic effect, the tilt angle induced by E in chiral compounds, is $\approx 20°/(\mathrm{V}/\mu\mathrm{m})$. See M. S. Spector, P. A. Heiney, J. Naciri, B. T. Weslowski, D. B. Holt, and R. Shashidhar, Phys. Rev. E **61**, 1579 (2000).

[11] One notices that the dielectric anisotropy under dc E is different from the one at optical frequency.

[12] D. W. Berreman, J. Opt. Soc. Am. **62**, 502 (1972).

[13] P. M. Johnson, D. A. Olson, S. Pankratz, Ch. Bahr, J. W. Goodby, and C. C. Huang, Phys. Rev. E **62**, 8106 (2000).

[14] We have checked the layer spacing in the Sm A phase determined by our NTE method against high-resolution x-ray diffraction of several liquid crystal compounds. The agreement of data obtained from these two methods is very well within the resolution of our NTE method. One of such comparisons has been made by C. C. Huang, S. T. Wang, X. F. Han, A. Cady, R. Pindak, W. Caliebe, K. Ema, K. Takekoshi, and H. Yao, Phys. Rev. E **69**, 041702 (2004).

[15] Recent studies have revealed that the Sm A_{db} phase of bulk samples of 1g14 is antiferroelectric, which was not reported in Ref. [8].

[16] A. Aharony, R. J. Birgeneau, J. D. Brock, and J. D. Litster, Phys. Rev. Lett. **57**, 1012 (1986); J. D. Brock, D. Y. Noh, B. R. McClain, J. D. Litster, R. J. Birgeneau, A. Aharony, P. M. Horn, and J. C. Liang, Z. Phys. B: Condens. Matter **74**, 197 (1989).

[17] A. Houghton and F. J. Wegner, Phys. Rev. A **10**, 435 (1974).

[18] J. Cardy, *Scaling and Renormalization in Statistical Physics* (Cambridge University Press, Cambridge, UK, 1996).

[19] The critical exponent of the optical biaxiality through the uniaxial Sm A to C_M transition was obtained to be 0.79 and 0.56 from bulk samples [3]. The measured values were attributed to the geometrical feature in the phase diagram of the binary mixture [3].